JOURNAL OF BACTERIOLOGY, Feb. 1994, p. 1060–1068
0021-9193/94/$04.00+0

Vol. 176, No. 4

Root Nodulation of *Sesbania rostrata*

IBRAHIMA NDOYE,[1]† FRANÇOISE DE BILLY,[2] JACQUES VASSE,[2] BERNARD DREYFUS,[1] AND GEORGES TRUCHET[2]*

Laboratoire de Microbiologie des Sols, Institut Français de Recherche Scientifique pour le Développement en Coopération (ORSTOM), Dakar, Sénégal,[1] and Laboratoire de Biologie Moléculaire des Relations Plantes-Microorganismes, Centre National de la Recherche Scientifique-Institut National de la Recherche Agronomique, 31326 Castanet-Tolosan Cédex, France[2]

Received 8 September 1993/Accepted 2 December 1993

The tropical legume *Sesbania rostrata* can be nodulated by *Azorhizobium caulinodans* on both its stem and its root system. Here we investigate in detail the process of root nodulation and show that nodules develop exclusively at the base of secondary roots. Intercellular infection leads to the formation of infection pockets, which then give rise to infection threads. Concomitantly with infection, cortical cells of the secondary roots dedifferentiate, forming a meristem which has an "open-basket" configuration and which surrounds the initial infection site. Bacteria are released from the tips of infection threads into plant cells via "infection droplets," each containing several bacteria. Initially, nodule differentiation is comparable to that of indeterminate nodules, with the youngest meristematic cells being located at the periphery and the nitrogen-fixing cells being located at the nodule center. Because of the peculiar form of the meristem, *Sesbania* root nodules develop uniformly around a central axis. Nitrogen fixation is detected as early as 3 days following inoculation, while the nodule meristem is still active. Two weeks after inoculation, meristematic activity ceases, and nodules then show the typical histology of determinate nodules. Thus, root nodule organogenesis in *S. rostrata* appears to be intermediate between indeterminate and determinate types.

Bacteria of the genera *Rhizobium*, *Bradyrhizobium*, and *Azorhizobium* are able to induce the formation of nitrogen-fixing nodules on leguminous plants. Nodulation is a highly complex process involving a succession of interactions between the host plant and the bacterium, from initial recognition and infection to nodule development and nodule function (5, 8, 14, 20, 22).

There are two main types of nodule development, the so-called indeterminate and determinate types (5, 14, 22, 24). Indeterminate nodules generally develop on temperate legumes, such as alfalfa, vetch, or pea. In these plants, the infection process occurs via root hairs and results in the formation of rhizobium-containing infection threads, which grow towards the root cortex (8, 33, 42). Simultaneously with infection, inner root cortical cells dedifferentiate to form a nodule primordium and then a nodule meristem (11, 14, 19). The persistent activity of the meristem, located at the outer extremity of the nodule, ensures nodule elongation for a number of weeks (41). While the meristem is active, rhizobia are released from the infection threads into the plant cell cytoplasm (5, 14, 17, 24). The differentiation of both symbionts leads to the establishment of a central zone of the nodule, in which nitrogen is reduced (22, 41). Thus, in indeterminate nodules, nodule growth and functioning occur simultaneously, and all intermediates in differentiation can be observed in a single longitudinal section of a nodule.

Determinate nodules are characteristic of tropical legumes. In legumes such as *Arachis hypogaea* and *Stylosanthes* spp., microsymbionts infect their hosts by "crack entry," i.e., intercellularly between adjacent cells without the formation of infection threads (1, 6, 7, 33). In other tropical legumes, such as *Glycine max* (26, 39), the infection process proceeds as in temperate legumes, i.e., by the formation of infection threads through root hairs. In tropical legumes, the nodule meristem is induced in the outer cortex, and the bacteria are released into actively dividing meristematic cells, each daughter cell receiving rhizobia (24, 26). Meristematic activity is restricted to a short period of time and, following a round of successive divisions, the invaded meristematic cells differentiate simultaneously to form the nitrogen-fixing central tissue (24). As a result of this developmental pathway, nodule growth and functioning are dissociated. Determinate nodules do not elongate but enlarge, and only a single stage of plant and bacterial differentiation can be observed at any particular moment in time.

Sesbania rostrata is one of the few legumes that forms nodules on both stems and roots (9). Until now, only stem nodule ontogeny has been studied in detail (9, 12, 38); a brief report has dealt with root nodulation (27). The formation of stem nodules by *Azorhizobium caulinodans* is induced following crack-entry infection at the base of dormant root primordia, which are present in rows along the length of the stem (38). Direct intercellular infection is followed by very active multiplication of the bacteria, forming wide intercellular spaces filled with azorhizobia. These azorhizobium-filled spaces then extend inward as narrow, branched, intercellular infection threads which spread into the meristematic zone induced in the cortex (12, 38). The subsequent release of bacteria into the cytoplasm of newly induced meristematic cells leads eventually to the development of a determinate nodule (12, 38). It has been reported that infection occurs by means of infection threads through root hairs during root nodulation of *S. rostrata*, (27), although other symbiotic steps were not addressed in that study.

We have investigated *S. rostrata* root nodule organogenesis. In this report, we describe root nodule formation and compare this nodulation process with that occurring on the stem. We

* Corresponding author. Mailing address: Laboratoire de Biologie Moléculaire, CNRS-INRA, BP 27, 31326 Castanet-Tolosan Cédex, France. Phone: (33) 61 28 50 51. Fax: (33) 61 28 50 61.

† Present address: Département de Biologie Végétale, Université Cheikh Anta Diop, Dakar, Sénégal.

find that root nodulation occurs through successive steps, some of which are unusual in character, and corresponds to a developmental program intermediate between indeterminate and determinate types.

MATERIALS AND METHODS

Bacterial strains and media. *A. caulinodans* ORS571, originally isolated from stem nodules of *S. rostrata* (10), was used as the inoculant. The strain was maintained on YL medium (10).

Plant culture and inoculation. For root nodulation tests, seeds were surface sterilized with concentrated H_2SO_4 for 60 min, washed three times with sterile distilled water, germinated on soft agar medium for 24 h at 30°C, and transferred aseptically to test tubes with Jensen's nitrogen-free medium on agar slants (43). The shoot was allowed to grow out of the tube, which was closed with an aluminum foil cap. Seedlings were grown in a controlled-environment cabinet at 28°C, with 16 h of lighting per 24-h cycle. Two days after transfer, each seedling was inoculated with 0.1 ml of a bacterial culture that contained about 10^8 cells per ml.

Fixation and embedding. Root and nodule samples were collected as early as 12 h after inoculation, daily from days 1 through 7, and finally on days 10 and 14 postinoculation. Root nodules of *S. rostrata* were fixed in glutaraldehyde (2.75% in 0.2 M sodium cacodylate buffer [pH 7.2]) for 30 min under vacuum and 90 min at atmospheric pressure, washed three times for 60 min each time in sodium cacodylate (0.3 M; pH 7.2), and postfixed for 1 h in osmium tetroxide (1% in 0.3 M sodium cacodylate buffer [pH 7.2]). Fixed samples were rapidly washed with distilled water, dehydrated through graded ethanol solutions, and embedded in Epon.

Light microscopy. Light microscopy was performed on whole root systems, on slices of nonembedded nodules, or on semithin sections of embedded samples.

Whole root systems were fixed in glutaraldehyde as described above, rapidly washed with distilled water, and cleared in a solution of sodium hypochlorite (34). After clearing, samples were rinsed in distilled water, stained for 5 min with methylene blue (0.01% in distilled water) (42), and observed by bright-field microscopy with an Olympus Vanox light microscope.

Longitudinal slices (80 to 100 μm thick) were obtained from fixed nodules. Slices were fixed again in 2.75% glutaraldehyde for 15 min, cleared, stained, and observed as described above.

Epon-embedded samples were cut on a Reichert Jung ultramicrotome. Semithin sections (0.9 μm) were laid on a slide and stained by the basic fuchsin-methylene blue method (15) before observation by bright-field microscopy.

Transmission electron microscopy. Ultrathin sections of fixed and embedded nodules were cut on a Reichert Jung ultramicrotome, mounted on Formvar membrane grids, and stained with uranyl acetate and then lead citrate (28). A Hitachi EM 600 transmission electron microscope operating at 75 kW was used to examine the ultrathin sections.

RESULTS

Nodules develop at the base of lateral roots. The root system of *S. rostrata* grown in test tubes possesses a main tap root, out of which emerge numerous lateral roots. For noninoculated plants, only a few thin root hairs developed on the visible part of the lateral root. However, 12 h following inoculation with *A. caulinodans* ORS571, short and thick root hairs appeared at the base of the lateral root, i.e., on the part which lies in the cortex of the tap root. At 16 h after inoculation, this part of the lateral root was seen to swell. These two features were easily seen 48 h postinoculation, particularly after the removal of the cortex from roots previously cleared with sodium hypochlorite (Fig. 1A and B). The fact that, for older inoculated plants, nodulation sites were exclusively restricted to the base of the lateral root, which lies hidden within the tap root cortex, confirmed that swellings corresponded to centers of inner meristematic activity (Fig. 1B).

Infection process: intercellular infection, infection pockets, and infection threads. Despite a detailed observation of whole plants, we could detect neither root hair curling (shepherd's crooks) nor the development of infection threads at the apex of root hairs induced in the nodulation region. However, infection was observed as early as 16 h after inoculation within the swollen region at the base of lateral roots. For whole plants, we were able to observe, albeit infrequently, that the infection process was intercellular in character and that infection occurred at the point of contact between two cells (e.g., between two root hairs, a root hair and an epidermal cell, or two adjacent epidermal cells) (Fig. 1C). Light microscopy of semithin sections of developing nodules confirmed that the infection proceeded intercellularly (Fig. 1D and E) and revealed the presence of infection pockets extending inward over a distance of two or three plant cell layers (Fig. 1F to I). Ultrastructurally, the infection pockets appeared to be filled with proliferating azorhizobia embedded in a moderately electron-dense matrix (data not shown). Later, during nodule ontogeny, narrow infection threads originated from the infection pockets (Fig. 1G and I and 2A) and grew towards the meristematic cells induced in the plant cortex (see below).

Peculiar "open-basket" shape of the *Sesbania* root nodule meristem. The nodule meristem originated within the root middle and inner cortical cell layers before bacterial infection had progressed beyond the most peripheral root cells (Fig. 1D). At 16 to 24 h after inoculation, the meristem appeared as a condensed spherical structure positioned opposite the site of infection (Fig. 1D). However, by 24 to 48 h after inoculation, the meristem had evolved into a shape best described as a 360° open-basket structure, entirely enveloping the initial infection site (Fig. 1F and H). As a result of this unusual location of the meristem, the nodule enlarged equally in all directions and thus extended in width rather than in length.

Nodule differentiation displays characteristics of both indeterminate and determinate nodules. Infection threads, which originated from infection pockets, first grew towards the newly induced meristem (Fig. 2A) and then extended in all directions following the peripheral enlargement of the meristem (Fig. 2B). During the first week following inoculation, the growth of the nodule and the differentiation of the central tissue occurred simultaneously. Histologically, the central tissue of developing *S. rostrata* root nodules comprises three main zones: an actively dividing nodule meristem located at the periphery, an intermediary zone enriched with infection threads, and a central region corresponding to the nitrogen-fixing zone (Fig. 2B). This histological organization is very similar to that of indeterminate nodules, in which the youngest tissues are located at the growing tip of the nodule and the most differentiated tissues are found near the nodule center (41). However, in contrast to indeterminate nodules, which display a longitudinal gradient of cell differentiation (41), developing *S. rostrata* root nodules presented a lateral gradient around the original infection site. This difference is a reflection of the shape and the direction of growth of the two types of meristems. Finally, it is worth noting that nitrogen fixation, assayed by acetylene reduction, started as early as 3 days after

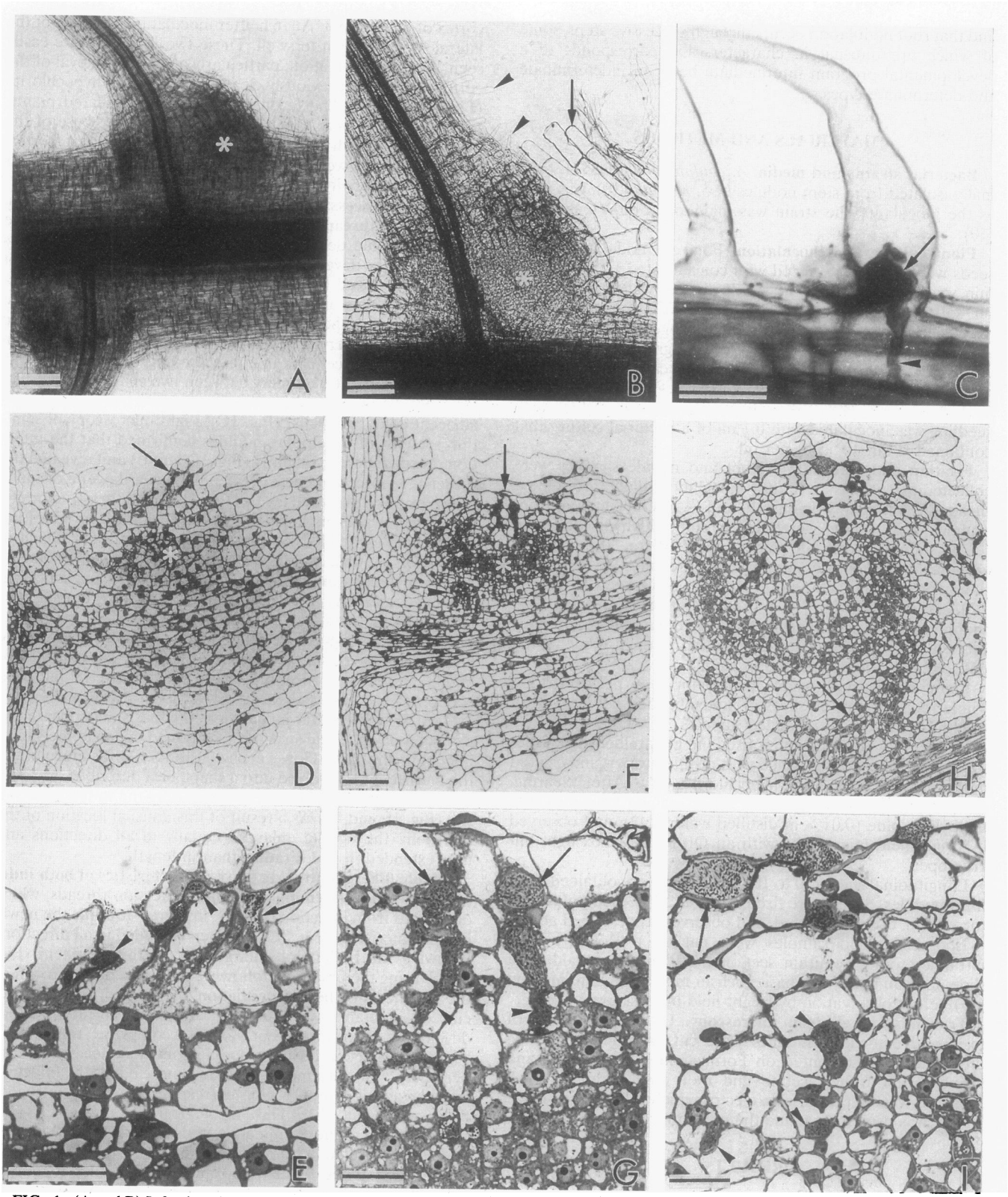

FIG. 1. (A and B) Infection sites 48 h after inoculation. Light microscopy of whole root systems of *S. rostrata* cleared with sodium hypochlorite before dissection (A) or after removal (B) of the tap root cortex. The slight swellings (asterisks) at the base of lateral roots reflect meristematic activity. In panel B, the arrowheads point to root hairs which have developed on the hidden region of the lateral root, and the arrow shows remnants of the main root cortex after dissection. Bars, 100 μm. (C to I) Infection process and meristem induction. (C) Whole plant stained with methylene blue 16 h after inoculation. Intercellular infection is taking place at the contact point of two adhering root hairs. An infection pocket (arrow) and an infection thread (arrowhead) can be seen. (D to I) Semithin sections (2-μm width) of nodules fixed 16 h (D and E), 24 h (F and G), and 36 h (H and I) after inoculation. (D) Meristem induction in relation to the infection site (arrow). Cortical cells (asterisk) divide before

inoculation, i.e., when developing nodules first showed a pink coloration. The fact that acetylene reduction increased dramatically from days 3 to 9 (data not shown) is strong evidence that nitrogen fixation is due to symbiotic rather than free-living bacteria.

Nodule development came to a halt approximately 8 to 10 days after inoculation, presumably because of the arrest of meristematic activity. Mature nodules, 2 to 3 weeks after inoculation, were oval in shape, reflecting the peripheral growth of the nodules (Fig. 2C). Mature nodules displayed the histological organization of determinate nodules, comprising a central region and peripheral tissues (Fig. 2C). The central region comprised both infected nitrogen-fixing cells and noninvaded cells (Fig. 2C and D). Interestingly, a central gap surrounded by the nitrogen-fixing tissue was persistent in the mature nodules (Fig. 2C), reflecting the position of the original site of infection. The peripheral tissues comprised an outer layer of sclerenchyma, nodule parenchyma cells, and vascular bundles surrounded by an endodermis (Fig. 2C and D). The vascular bundles, which started to differentiate as early as 24 h after inoculation (Fig. 1F), were connected with the plant vasculature (Fig. 1H and 2C).

Bacterial release: infection droplets. Ultrastructurally, infection threads, which originated from infection pockets, were surrounded by a cell wall and the plasmalemma of the plant cell (Fig. 3A). Bacterial release was initiated approximately 2 days after inoculation. At this stage, marked ultrastructural changes were observed, presumably at the tip of intracellular branches of infection threads. The cell wall was generally absent, and the embedding matrix was reduced, often displaying a patchy distribution (Fig. 3A). In these branches, electron-dense bacteria close to the wall-lacking tip exhibited an irregular shape and were only separated from the plant cell cytoplasm by the plasmalemma of the host cell (Fig. 3A and B). The fact that these structural features were seen in plant cells in which the first symbiosomes were eventually observed suggested that they were a prelude to plant cell invasion by azorhizobia. Such invasion could occur following release into the host cell cytoplasm of individual infection droplets, i.e., of the wall-lacking regions of infection threads (Fig. 3C). Each infection droplet was delimited by a plasmalemma-derived membrane, generally contained two or three bacteria, and was often filled with a moderately electron-dense material, most probably the remnant of the matrix in which the bacteria were embedded in the infection thread (Fig. 3A to C). Despite numerous observations, we did not obtain any ultrastructural evidence that bacterial release occurred by endocytosis either from infection threads or from infection droplets.

Ultrastructural differentiation of bacteroids. In contrast to the presence of several bacteria in infection droplets, only one bacteroid was seen in the first symbiosomes formed (Fig. 4A and B). At this stage of differentiation, there was evidence that each symbiosome divided, generating symbiosomes also containing one bacteroid (Fig. 4A to C). Ultrastructurally, the bacteroid appeared electron dense, and the peribacteroid membrane displayed an irregular shape, presumably because of the fusion of plant cytoplasmic vesicles containing a moderately electron-dense material (Fig. 4B). At a later stage, the more regular profile of the peribacteroid membrane could be correlated with a progressive reduction in the number of plant cytoplasmic vesicles (Fig. 4C). Each symbiosome contained one or two elongated, moderately electron-dense azorhizobia (Fig. 4C). This small increase in the number of bacteroids per symbiosome could have been the result of the fusion of peribacteroid membranes (Fig. 4C). Cytoplasmic vesicles were no longer observed in the most differentiated of the invaded plant cells, which appeared to be almost totally filled with large symbiosomes (Fig. 4D and E). Each symbiosome contained many electron-dense bacteroids characterized by a regular shape and the deposition of large poly-β-hydroxybutyrate granules in their cytoplasm (Fig. 4D and E). Ultrastructural observations showed that the bacteroids no longer divided in this zone of the nodule and substantiated the conclusion that the increase in the number of bacteroids per symbiosome was a consequence of the fusion of peribacteroid membranes (Fig. 4E). Ultimately, such fusions led to symbiosomes which displayed a rose-shaped configuration, each symbiosome containing a large number of bacteroids (compare Fig. 4E and D).

DISCUSSION

In certain respects, the root nodulation process in *S. rostrata* resembles that already described for other tropical legumes. For example, root nodule development at the base of the lateral root, i.e., in the region of the lateral root which lies in the tap root cortex, is common to various tropical legumes, including members of the genera *Arachis* (6), *Stylosanthes* (7), *Aeschynomene* (3, 23), and *Neptunia* (16, 30). In the case of temperate legumes, such as alfalfa or clover, a zone which corresponds to the region of root hair development is the preferred site for the initiation of nodulation (4).

On the other hand, what is remarkable about *Sesbania* root nodulation is that four developmental events, namely, the infection process, the spatiotemporal organization of the meristem, bacterial release, and the overall differentiation of the nodule, display a number of unusual features which, in certain cases, have not yet been described for other symbiotic associations.

Infection process. Root infection of *S. rostrata* by *Azorhizobium* spp. is a three-step process which includes intercellular infection (crack entry), the formation of large intercellular infection pockets in which bacteria divide actively and, finally, the development of infection threads, which originate from these infection pockets and then spread into the root cortex.

Intercellular invasion, which also characterizes the stem nodulation of *S. rostrata* (12, 38), is a feature common to a number of tropical legumes, including *A. hypogaea* (6), *Stylosanthes* spp. (7), *Aeschynomene indica* (3), *A. americana* (23), *Neptunia plena* (16), and *N. oleracea* (30). This mode of infection has also been described for alfalfa roots, which are normally infected through root hairs, following inoculation either with a strain of *Agrobacterium tumefaciens* carrying the

the infection has progressed beyond the outermost plant cells. (E) Magnification of panel D showing the intercellular infection occurring between two epidermal cells (arrow) or between adjacent root hairs (arrowheads). (F) Development of the nodule meristem (asterisk) into a 360° open-basket structure surrounding the infection site (arrow). The arrowhead points to nodule vascular bundles. (G) Magnification of panel F showing intercellular infection pockets (arrows) filled with azorhizobia and infection threads (arrowheads) originating from the infection pockets. (H) Typical aspect of the nodule meristem surrounding the original infection site (star). The arrow shows the connection between nodule vascular bundles and the plant stele. (I) Magnification of panel H showing the spread of the infection threads (arrowheads) originating from the infection pockets (arrows). Bars, 50 μm (C, E, G, and I) and 100 μm (D, F, and H).

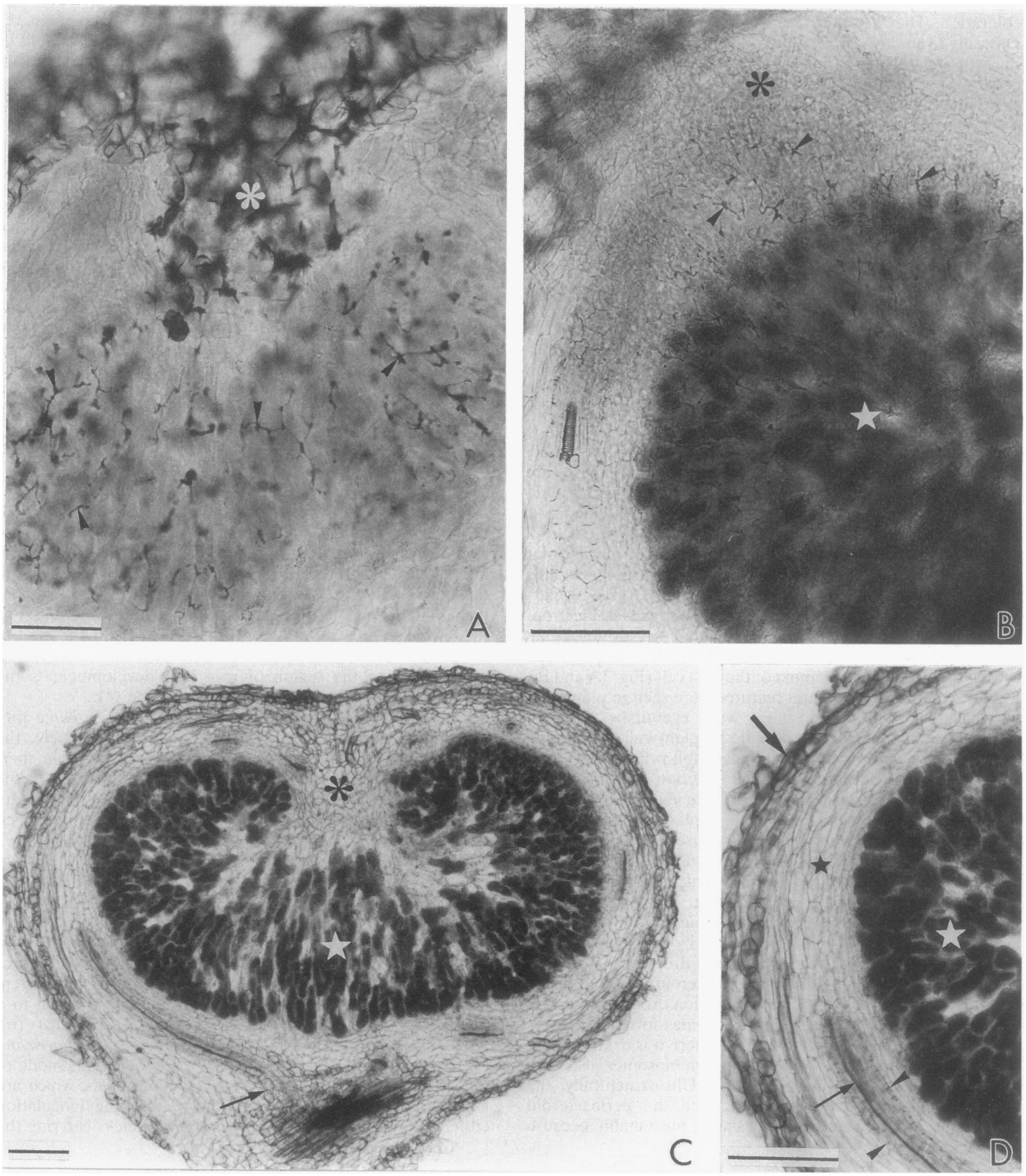

FIG. 2. Nodule differentiation. Light microscopy of 80-μm-thick sections of nodules stained with methylene blue and partially cleared with sodium hypochlorite. (A) Nodule fixed 48 h after inoculation illustrating the spread of infection threads (arrowheads) to the newly induced meristem. The asterisk indicates the infection site. (B) One-half of a 5-day-old nodule showing the meristem (asterisk), the infection threads (arrowheads), and the central nitrogen-fixing tissue (star). (C) Histology of a mature nodule, 2 weeks after inoculation. The nitrogen-fixing tissue of the nodule surrounds the original infection site (asterisk). The arrow shows the connection between the plant vasculature and nodule vascular bundles. (D) Magnification of panel C showing the peripheral tissues of a mature nodule: the sclerenchyma (large arrow), the nodule parenchyma (black star), and the endodermis (arrowheads) surrounding the vascular bundles (arrow). The nitrogen-fixing tissue (white star) comprises both invaded and noninvaded cells. Bars, 100 μm.

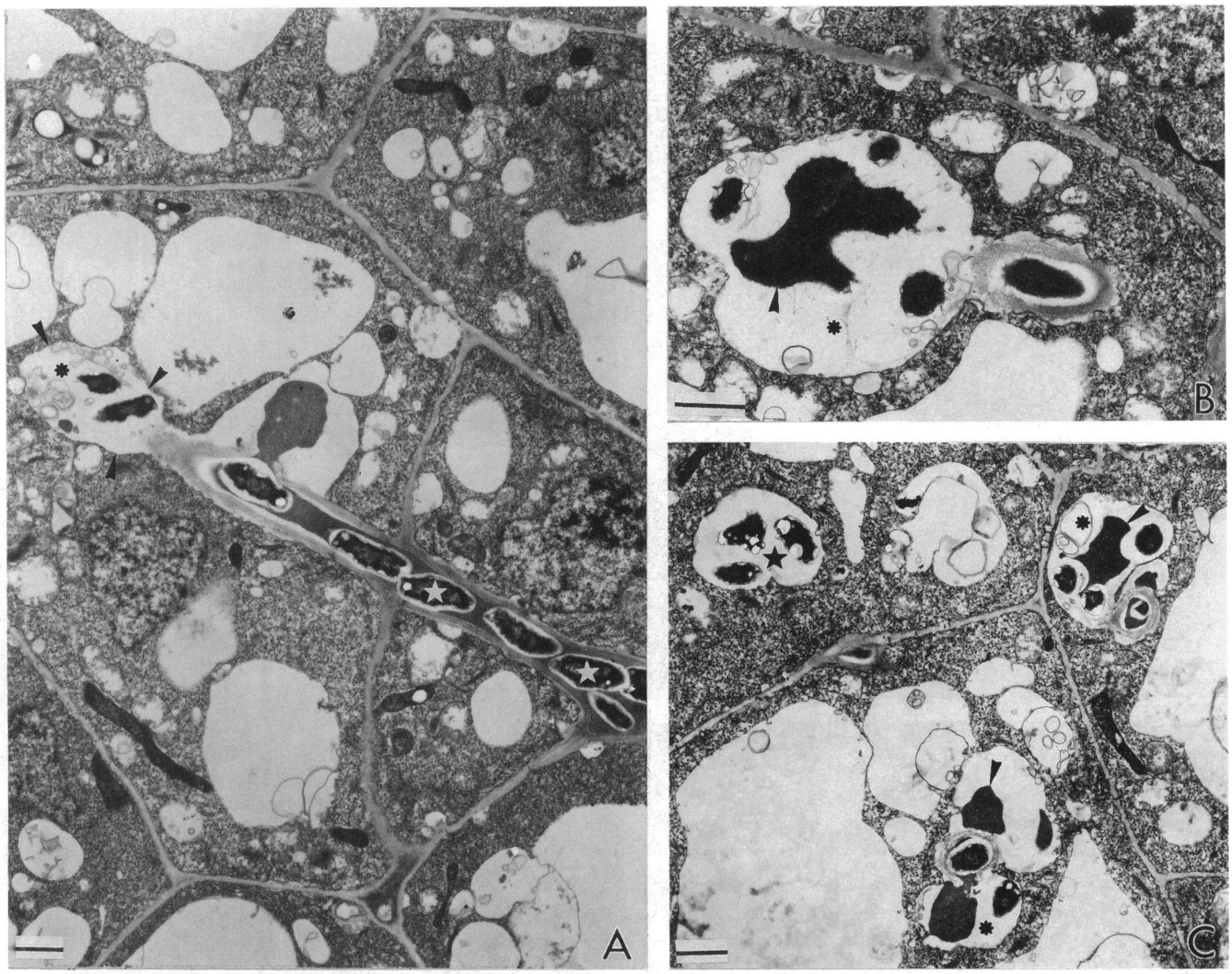

FIG. 3. Bacterial release. Transmission electron microscopy. (A) Infection thread penetrating into the plant cell cytoplasm. Bacteria (stars) are embedded in the matrix of the thread. Note the absence of the cellulose sheath at the tip of the infection thread (asterisk). Arrowheads point to the plasmalemma limiting the thread. (B and C) Infection droplets still attached to the thread (asterisks) or released into the plant cell cytoplasm (star). Bacteria and remnants of the matrix (arrowheads) can be seen in the infection droplets. Bars, 1 μm.

symbiotic plasmid of *Rhizobium meliloti* (37) or with an exopolysaccharide-deficient mutant of *R. meliloti* (13). As such, it can be considered a "primitive" type of infection.

The formation of infection pockets is visible as early as 12 h after inoculation. The infection pockets appear to be typical for the *S. rostrata* nodulation process because they have also been observed during stem nodulation of this plant (12, 38). To our knowledge, intercellular structures resembling the intercellular infection pockets described in this study have only been observed during nodule ontogenesis in *Neptunia* species (16, 30). In *N. plena* (16), bacteria accumulate in intercellular spaces of a smaller size. In *N. oleracea* (30), intercellular infection is followed by the formation of a "horn of plenty" in which bacteria proliferate.

During root nodulation of *S. rostrata*, infection threads, which originate from the intercellular infection pockets, are formed. This same feature also characterizes stem infection of this legume (12, 38) and infection of *Neptunia* species (16, 30). This process differs notably from the infection process described for *A. indica* (3) and *A. hypogaea* (6), for which neither intercellular pockets nor infection threads have been described. Following inoculation of *S. rostrata* roots with *A. caulinodans* ORS571 and despite numerous detailed observations, we were unable to observe infection threads in curled root hairs, as has been previously reported (27).

Spatiotemporal organization of the meristem. In *S. rostrata*, root nodule meristems are induced simultaneously with infection in middle and inner cortical cell layers. Thus, for this tropical legume, root nodules originate at the same histological level as indeterminate nodules of temperate legumes (11, 19, 26, 34, 36) and not from the root outer cortex, as for most tropical legumes (2, 6, 7, 26, 39). Moreover, by showing that nodule meristematic centers can be detected during the very first hours following inoculation, before infection has progressed beyond the outermost plant cells, our results suggest that the meristem is induced at a distance (35, 36). During the last decade, different groups have shown that nodulating rhizobia produce lipooligosaccharidic Nod factors (18, 32), which are able to induce inner cortical cell divisions (32, 36) and nodule development in alfalfa (36). More recently, it was

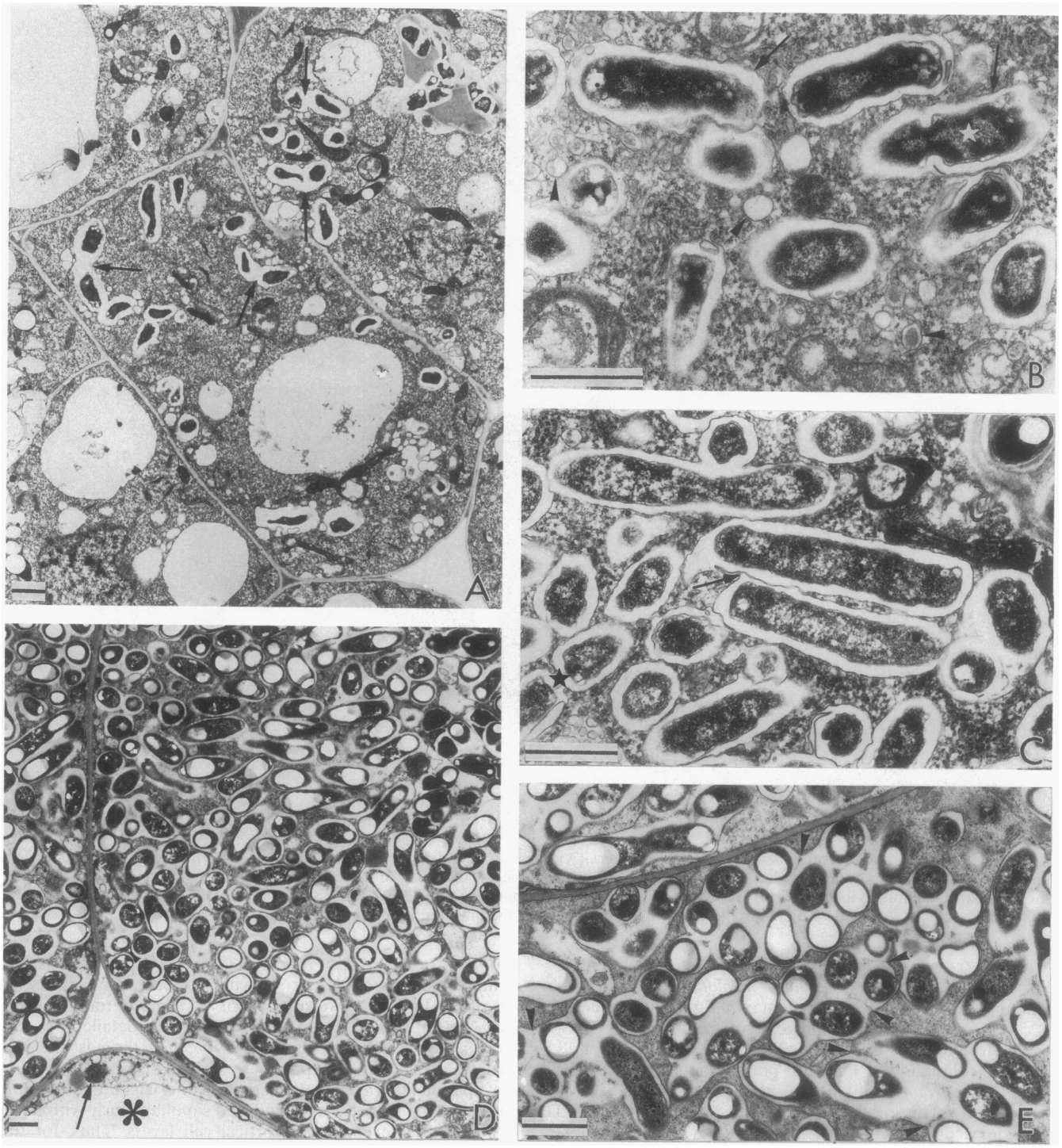

FIG. 4. Bacteroid differentiation. Transmission electron microscopy. (A and B) Newly formed symbiosomes. (A) The arrows point to dividing symbiosomes. (B) Magnification showing the presence of vesicles (arrowheads) in the plant cell cytoplasm and the irregular shape of the peribacteroid membranes (arrows). A bacteroid is dividing (star). (C) Elongated bacteroids. The arrow indicates a possible fusion of peribacteroid membranes. The star indicates a dividing symbiosome. (D) Invaded cells of the central tissue. Note the large number of symbiosomes per invaded cell and the deposition of large poly-β-hydroxybutyrate granules in bacteroids. A peroxisome (arrow) is seen in a noninvaded cell (asterisk). (E) Fusions of peribacteroid membranes (arrowheads) and the formation of symbiosomes containing a large number of bacteroids. Bars, 1 μm.

shown that *A. caulinodans* ORS571, the strain used as an inoculant in this study, also produces lipooligosaccharidic Nod factors (21). In *S. rostrata*, these factors elicit the division of cortical cells at the axils of lateral roots (21), i.e., at sites at which root nodulation occurs (this work).

The spatiotemporal organization of the nodule meristem changes drastically in the first few hours following its induction. Initially, the meristem appears as a mass of cells located proximal to, i.e., in front of, the site of infection. Later on, there is a uniform expansion of the meristem, which results in

the formation of an open-basket structure surrounding the initial infection site. To our knowledge, such an unusual organization for a nodule meristem has never been described.

Bacterial release. The release of azorhizobia in *S. rostrata* root nodules also proceeds in an unusual way. Infection droplets, each carrying one or more bacteria, are budded off in the plant cell cytoplasm from the wall-lacking tip of the infection thread. Similar infection droplets have been described for nodules of *N. plena* (16) and *Lotus corniculatus* (40). Infection droplets containing several bacteria have also been noted for *Vigna radiata* (25). Intriguingly, we have not been able to find an ultrastructural intermediate between the infection droplets, which most often contain more than one bacterium, and the symbiosomes, which at their earliest stage of differentiation contain only a single bacteroid. Moreover, the fact that we have never observed bacterial release by endocytosis raises the question of how the first symbiosomes are formed. One explanation could be that the first symbiosomes are formed by the compartmentalization of the plasmalemma-derived membrane that surrounds the original infection droplet into as many compartments as there are bacteria enclosed in the droplet. The division of each symbiosome, i.e., the simultaneous division of the bacteroid and its peribacteroid membrane, as described in this study, would then result in an increase in the number of symbiosomes, each one still containing a single bacteroid. Finally, because we have seen that the number of bacteroids enclosed in a single peribacteroid membrane increases during nodule differentiation and because no division of bacteroids in peribacteroid spaces has been observed, we hypothesize that such an increase results from frequent fusions between the peribacteroid membranes of adjacent symbiosomes. It is worth noting that for *V. radiata* (25), the release of bradyrhizobia from infection droplets occurs by an endocytotic mechanism similar to that described for many legumes (17, 26, 29).

Differentiation of the nodule. The shape of a nodule depends on the location and the period of activity of its meristem. In indeterminate nodules, the lengthy activity (several weeks) of the apical meristem is responsible for the elongation of the nodules (14, 24, 41). In *S. rostrata* root nodules, the activity of the peripheral meristem, restricted to a shorter period of time following inoculation, accounts for the uniform enlargement of the nodules, with the infected tissue surrounding the initial infection site. Indeed, the pattern of differentiation of the central tissue is very similar for both nodule types. Meristematic tissue, infection tissue, and inner tissue (in which nitrogen fixation occurs), which are observed successively from the outside of the *Sesbania* root nodule towards the infected tissue, are equivalent to the histological zones which differentiate along the axis of indeterminate nodules (41). This pattern of differentiation explains why two features typical of indeterminate nodules also characterize *S. rostrata* root nodule development: (i) all stages of symbiont differentiation can be observed at a single time point in sections of developing nodules (at least during the first week after inoculation), and (ii) nitrogen fixation takes place while the root nodules are still actively growing.

The meristematic activity which normally continues for many weeks in indeterminate nodules abruptly comes to a halt in 1-week-old *Sesbania* root nodules. At the end of the differentiation process, the root nodules of *S. rostrata* display the round shape and the overall histological organization of determinate nodules typical of most tropical legumes, such as *A. indica* (3), *A. hypogaea* (6), and *G. max* (26, 31), as well as of the stem nodules of *A. afraspera* (2) and *S. rostrata* (38).

Stem and root nodulation in *S. rostrata*. Certain similarities can be found when the nodulation processes which take place on the stem (12, 38) and on the root system (this work) of *S. rostrata* are compared. (i) In both cases, nodulation sites are restricted to cavities either surrounding dormant root primordia present all along the stem (9) or created on the tap root by emerging lateral roots (this work). However, there is no root hair induction at the stem nodulation site, such as that which is observed at the lateral root axil of plants inoculated with *A. caulinodans* ORS571 (this work) or treated with Nod factors produced by the same strain (21). (ii) The infection processes, involving intercellular infection and the formation of infection threads originating from infection pockets, are comparable. (iii) In both cases, the nodule meristem is induced in the cortex at a distance from the site of infection. (iv) Fully differentiated stem and root nodules are of the determinate type. Unfortunately, because there is no available information for stem nodulation concerning certain symbiotic steps, such as bacterial release, the organization of the meristem, and the early steps in nodule differentiation, it is not yet possible to determine whether the stem and root nodulation processes are fully identical in *S. rostrata*. It would be of particular interest to investigate whether the differentiation of *Sesbania* stem nodules is also intermediate between indeterminate and determinate types of nodule development.

ACKNOWLEDGMENTS

We are grateful to Janet Sprent, Julie Cullimore, Dave Barker, and Koen Goethals for critical reading of the manuscript and English corrections, and we thank Anna Marthe Konte for typing the manuscript.

This work was supported by a grant from the Commission of the European Communities (TS2-0135B).

REFERENCES

1. **Alazard, D., and E. Duhoux.** 1990. Development of stem nodules in a tropical forage legume, *Aeschynomene afraspera*. J. Exp. Bot. **41**:1199–1206.
2. **Allen, O. N., and E. K. Allen.** 1940. Response of the peanut plant to inoculation with rhizobia, with special reference to morphological development of the nodules. Bot. Gaz. (Chicago) **102**:121–142.
3. **Arora, N.** 1954. Morphological development of the root and stem nodules of *Aeschynomene indica* L. Phytomorphology **4**:211–216.
4. **Bhuwaneswari, T. V., A. A. Baghwat, and W. D. Bauer.** 1981. Transient susceptibility of root cells in four legumes to nodulation by rhizobia. Plant Physiol. **68**:1144–1149.
5. **Brewin, N. J.** 1991. Development of the legume root nodule. Annu. Rev. Cell Biol. **7**:191–226.
6. **Chandler, M. R.** 1978. Some observations on the infection of *Arachis hypogaea* L. by *Rhizobium*. J. Exp. Bot. **29**:749–755.
7. **Chandler, M. R., R. A. Date, and R. J. Roughley.** 1982. Infection and root nodule development in *Stylosanthes* species by *Rhizobium*. J. Exp. Bot. **33**:47–57.
8. **Dénarié, J., F. Debellé, and C. Rosenberg.** 1992. Signalling and host range variation in nodulation. Annu. Rev. Microbiol. **46**:497–531.
9. **Dreyfus, B. L., and Y. R. Dommergues.** 1981. Nitrogen-fixing nodules induced by *Rhizobium* on the stem of the tropical legume *Sesbania rostrata*. FEMS Microbiol. Lett. **10**:313–317.
10. **Dreyfus, B. L., J. L. Garcia, and M. Gillis.** 1988. Characterization of *Azorhizobium caulinodans* gen. nov., sp. nov., a stem-nodulating nitrogen-fixing bacterium isolated from *Sesbania rostrata*. Int. J. Syst. Bacteriol. **38**:89–98.
11. **Dudley, M. E., T. W. Jacobs, and S. R. Long.** 1987. Microscopy studies of cell division induced in alfalfa roots by *Rhizobium meliloti*. Planta **171**:289–301.
12. **Duhoux, E.** 1984. Ontogénèse des nodules caulinaires de *Sesbania rostrata* (légumineuse). Can. J. Bot. **62**:982–994.
13. **Finan, T. M., A. M. Hirsch, J. A. Leigh, E. Johansen, G. A. Kuldau,**

S. Deegam, G. C. Walker, and E. R. Signer. 1985. Symbiotic mutants of *Rhizobium meliloti* that uncouple plant from bacterial differentiation. Cell **40**:869–877.

14. **Hirsch, A. M.** 1992. Developmental biology of legume nodulation. New Phytol. **122**:211–237.
15. **Huber, J. D., F. Parker, and G. F. Odland.** 1968. A basic fuchsin and alkalinized methylene blue rapid stain for epoxy embedded tissue. Stain Technol. **43**:83–87.
16. **James, E. K., J. I. Sprent, J. M. Sutherland, S. G. McInroy, and F. R. Minchin.** 1992. The structure of nitrogen fixing root nodules on the aquatic mimosoid legume *Neptunia plena*. Ann. Bot. **69**:173–180.
17. **Kijne, J. W.** 1975. The fine structure of pea root nodule. 1. Vacuolar changes after endocytotic host cell infection by *Rhizobium leguminosarum*. Physiol. Plant Pathol. **5**:75–79.
18. **Lerouge, P., P. Roche, C. Faucher, F. Maillet, G. Truchet, J.-C. Promé, and J. Dénarié.** 1990. Symbiotic host-specificity of *Rhizobium meliloti* is determined by a sulphated acylated glucosamine oligosaccharide signal. Nature (London) **344**:781–784.
19. **Libbenga, K. R. F., and P. A. A. Harkes.** 1973. Initial proliferation of cortical cells in the formation of root nodules in *Pisum sativum*. Planta **114**:17–28.
20. **Long, S. R.** 1989. *Rhizobium*-legume nodulation: life together in the underground. Cell **56**:203–214.
21. **Mergaert, P., M. van Montagu, J.-C. Promé, and M. Holsters.** 1993. Three unusual modifications, a D-arabinosyl, an N-methyl, and a carbamoyl group, are present on the Nod factors of *Azorhizobium caulinodans* strain ORS571. Proc. Natl. Acad. Sci. USA **90**:1551–1555.
22. **Nap, J. P., and T. Bisseling.** 1990. Developmental biology of a plant-prokaryote symbiosis: the legume root nodule. Science **250**: 948–954.
23. **Napoli, C., F. Dazzo, and D. Hubbel.** 1975. Production of cellulose microfibrils by *Rhizobium*. Appl. Microbiol. **30**:123–131.
24. **Newcomb, W.** 1981. Nodule morphogenesis and differentiation, p. 247–298. *In* K. L. Giles and A. G. Atherly (ed.), Biology of *Rhizobiaceae*. Academic Press, Inc., New York.
25. **Newcomb, W., and L. McIntyre.** 1981. Development of root nodules of mungbean (*Vigna radiata*): a reinvestigation of endocytosis. Can. J. Bot. **59**:2478–2499.
26. **Newcomb, W., D. Spippell, and R. L. Peterson.** 1979. The early morphogenesis of *Glycine max* and *Pisum sativum* root nodules. Can. J. Bot. **57**:2603–2616.
27. **Olsson, J. E., and B. G. Rolfe.** 1985. Stem and root nodulation of the tropical legume *Sesbania rostrata* by *Rhizobium* strains ORS-571 and WE7. J. Plant Physiol. **121**:199–210.
28. **Reynolds, E. S.** 1963. The use of lead citrate at high pH as an electron opaque stain in electron microscopy. J. Cell Biol. **17**:208–213.
29. **Robertson, J. G., P. Lyttleton, S. Bullivant, and G. F. Grayston.** 1978. Membranes in lupin root nodules. The role of Golgi bodies in the biogenesis of infection threads and peribacteroid membranes. J. Cell Sci. **30**:129–149.
30. **Schaede, R.** 1940. Die Knollchen der adventiven Wasserwurzeln von *Neptunia oleracea* und ihre Bakteriensymbiose. Planta **31**:1–21.
31. **Selker, J. M. L., and E. H. Newcomb.** 1985. Spatial relationships between uninfected and infected cells in root nodules of soybean. Planta **165**:446–454.
32. **Spaink, H. P., D. M. Sheeley, A. A. N. van Brussel, J. Glushka, W. S. York, T. Tak, O. Geiger, E. P. Kennedy, V. N. Reinhold, and B. J. J. Lugtenberg.** 1991. A novel highly unsaturated fatty acid moiety of lipo-oligosaccharide signals determines host specificity of *Rhizobium*. Nature (London) **354**:125–130.
33. **Sprent, J. I., and S. M. Faria.** 1988. Mechanisms of infection of plants by nitrogen fixing organisms. Plant Soil **110**:157–165.
34. **Truchet, G., S. Camut, F. de Billy, R. Odorico, and J. Vasse.** 1989. The *Rhizobium*-legume symbiosis: two methods to discriminate between nodules and other root-derived structures. Protoplasma **149**:82–88.
35. **Truchet, G., M. Michel, and J. Dénarié.** 1980. Sequential analysis of the organogenesis of lucerne (*Medicago sativa*) root nodules using symbiotically-defective mutants of *Rhizobium meliloti*. Differentiation **16**:163–172.
36. **Truchet, G., P. Roche, P. Lerouge, J. Vasse, S. Camut, F. de Billy, J.-C. Promé, and J. Dénarié.** 1991. Sulfated lipo-oligosaccharide signals of *Rhizobium meliloti* elicit root nodule organogenesis in alfalfa. Nature (London) **351**:660–673.
37. **Truchet, G., C. Rosenberg, J. Vasse, J.-S. Julliot, S. Camut, and J. Dénarié.** 1984. Transfer of *Rhizobium meliloti* pSym genes into *Agrobacterium tumefaciens*: host-specific nodulation by atypical infection. J. Bacteriol. **157**:134–142.
38. **Tsien, H. C., B. L. Dreyfus, and E. L. Schmidt.** 1983. Initial stages in the morphogenesis of nitrogen-fixing stem nodules of *Sesbania rostrata*. J. Bacteriol. **156**:888–897.
39. **Turgeon, B. G., and W. D. Bauer.** 1985. Ultrastructure of infection thread development during the infection of soybean by *Rhizobium japonicum*. Planta **163**:328–349.
40. **Vance, C. P., L. E. Johnson, S. Stade, and G. R. Groat.** 1982. Birdsfoot trefoil (*Lotus corniculatus*) root nodules: morphogenesis and the effect of forage harvest on structure and function. Can. J. Bot. **60**:505–518.
41. **Vasse, J., F. de Billy, S. Camut, and G. Truchet.** 1990. Correlation between ultrastructural differentiation of bacteroids and nitrogen fixation in alfalfa nodules. J. Bacteriol. **172**:4296–4306.
42. **Vasse, J., and G. Truchet.** 1984. The *Rhizobium*-legume symbiosis: observation of root infection by bright-field microscopy after staining with methylene blue. Planta **161**:487–489.
43. **Vincent, J. M.** 1970. A manual for the practical study of root-nodule bacteria. International Biological Programme handbook no. 15. Blackwell Scientific Publications Ltd., Oxford.